AIP | The Journal of Chemical Physics

Study of the chemiluminescent reaction between alkali dimers and oxygen atoms

H. Figger, R. Straubinger, and H. Walther

Citation: The Journal of Chemical Physics **75**, 179 (1981); doi: 10.1063/1.441820
View online: http://dx.doi.org/10.1063/1.441820
View Table of Contents: http://scitation.aip.org/content/aip/journal/jcp/75/1?ver=pdfcov
Published by the AIP Publishing

Study of the chemiluminescent reaction between alkali dimers and oxygen atoms

H. Figger and R. Straubinger

Projektgruppe für Laserforschung der Max-Planck-Gesellschaft zur Förderung der Wissenschaften e. V., D-8046 Garching, Federal Republic of Germany

H. Walther

Sektion Physik der Universität München and Projektgruppe für Laserforschung der Max-Planck-Gesellschaft zur Förderung der Wissenschaften e. V., D-8046 Garching, Federal Republic of Germany

(Received 2 January 1981; accepted 9 February 1981)

The reaction of alkali dimers with oxygen atoms has been studied in a crossed beam experiment. Strong chemiluminescence of the reaction products was observed. It is shown that the luminescence was emitted by alkali atoms from the reaction $M_2 + O \rightarrow MO + M^*$ (M alkali atom). M^* can be excited up to the exoergicity of this reaction at least in the cases M = Cs and Na. For M = Cs, detailed rate constants for the excitation of the different excited states have been determined using both laser induced fluorescence and chemiluminescence. The rates decrease nearly exponentially as a function of the excitation energy. They partly follow the expectation of statistical theories. Absolute reaction cross sections have been determined for all of the reactions investigated. They agree partially with those predicted by the harpoon model.

INTRODUCTION

Emission of the sodium *D* lines is observed from the upper layers of the earth's atmosphere in twilight as well as during the night. Among the various excitation mechanisms proposed to explain the origin of this radiation, chemiluminescence seems to be the most probable. So some authors assumed that sodium particles react with oxygen atoms or molecules in the atmosphere and as a result sodium atoms excited in the process emit the *D* light.[1,2]

So far the experimental and theoretical investigations of the alkali–oxygen system have given no clear results. Ogawa[2] made flow tube experiments where the reaction $Na_2 + O_2, O$ was studied. In this experiment no luminescence was observed. However, Golomb, Hoffman, and Best[3] report the emission of the Na *D* lines when sodium was released at night from a rocket at a height of 150 km. Their interpretation was that the sodium dimers formed when the material was ejected and reacted with atmospheric oxygen

$$Na_2 + O \rightarrow NaO + Na^* , \qquad (1)$$

or perhaps a two step reaction took place

$$Na_2 + O \rightarrow Na + NaO ,$$
$$NaO + O \rightarrow O_2 + Na^* , \qquad (2)$$

the Na^* emitting the fundamental *D* lines.

Struve *et al.*, using potential surface models,[4,5] compared Reaction (1) to the analogous ones

$$M_2 + X \rightarrow MX + M^* , \qquad (3)$$

where M = alkali atoms and X = halogen atoms. They conclude that the NaO product molecule is excited to the $^2\Sigma$ electronic state, emitting ($^2\Sigma \rightarrow {}^2\Pi$) in the infrared, while the product atom should be predominantly in its ground state.

In this paper experiments are described which have been undertaken to clarify this situation. A molecular alkali beam generated by expansion of alkali vapor through a nozzle was crossed with a beam of ground state oxygen atoms.

EXPERIMENTAL SETUP

A schematic diagram of the experiment is shown in Fig. 1. The vacuum vessel was pumped by a cryopump. The alkali supersonic beam was produced by an oven with two chambers separately heated by thermocoax wire. The temperature of the nozzle chamber was kept 50 K higher than that of the main chamber containing the alkali metal supply to prevent clogging of the opening (the nozzle throat diameter was 0.2 mm). The beam defining collimator (aperture diameter 5 mm, distance from the nozzle 30 mm) was heated for the same reason. The oven temperature was chosen as to maintain 100 Torr of alkali vapor pressure in the oven chamber, resulting in a beam intensity of about 10^{16} particles $cm^{-2} s^{-1}$

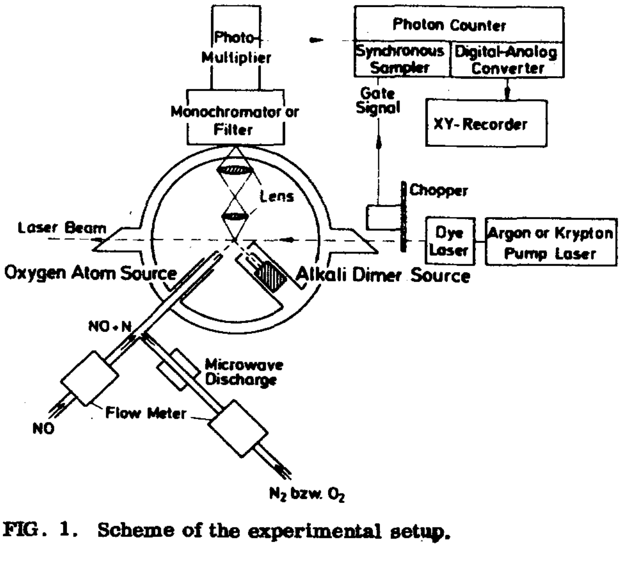

FIG. 1. Scheme of the experimental setup.

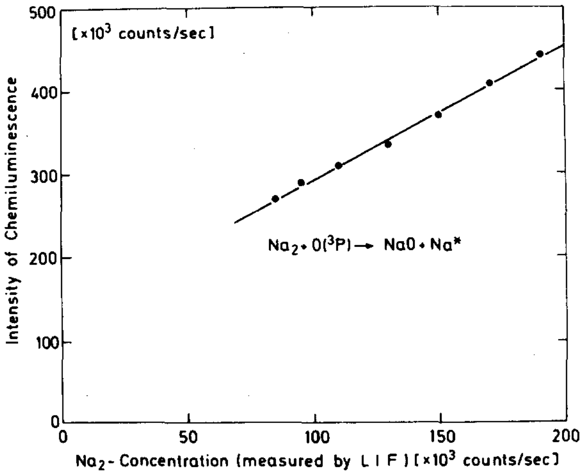

FIG. 2. Chemiluminescence intensity as a function of the dimer density in the supersonic sodium beam. The dimer density was measured by LIF using the dye laser.

at the reaction zone. The dimer fraction in the beam was about 10% as measured by laser induced fluorescence.

The beam of oxygen atoms which was crossed with the alkali beam was produced at first by a microwave discharge in O_2 flowing through a quartz tube whose exit hole had a diameter of 2 mm. It is well known that besides oxygen atoms and molecules in their ground states, species in metastable excited states leave such a source. The metastable species can transfer energy to the alkali beam, which consequently emits light. Therefore, we repeated all experiments with another type of oxygen source in which the rapid reaction

$$N + NO \rightarrow N_2 + O(^3P) \qquad (4)$$

was used. This reaction is usually applied for the titration of nitrogen atoms in the gas phase.[6] In this way, it was guaranteed that only ground state oxygen atoms were produced. The nitrogen atoms needed to initiate this reaction are generated by a microwave discharge in N_2. The $O(^3P)$ flux is equal to the NO flux which was measured by a flow meter. Its intensity was typically 3×10^{16} cm^{-2} s^{-1} at the reaction zone. Both types of O sources gave very similar results.

Chemiluminescence or laser induced fluorescence produced in the reaction zone was focused by a quartz lens system on the entrance slit of a 25 cm monochromator (Jobin-Yvon M 25). Its resolving power $\lambda/\Delta\lambda$ was 400 when the slit width was 0.25 mm. The light intensity was measured by a photomultiplier tube (RCA C 31034 B) together with a photon counting system (Brookdeal 5 C 1). For the laser induced fluorescence experiments, a cw single mode dye laser pumped by a krypton laser was used.

EXPERIMENTS AND RESULTS

In the crossed beam experiment, strong luminescence from the reaction zone is observed. The wavelength of the light corresponds to the fundamental *D* lines in the case of Na. We assume, in accordance with Golomb *et al.*,[3] that the luminescence is produced by the reaction mechanism

$$M_2 + O(^3P) \rightarrow MO + M^* , \qquad (5)$$

where M = an alkali atom, and where the excited atom M* emits the light. Two step reactions according to Reaction (2) can be excluded since beam densities and background pressure only allow single collisions. In order to show that M_2 is involved in the reaction and not M, we varied the M_2 density in the alkali beam by heating up the nozzle chamber while leaving the temperature of the other parts of the oven constant.[7] Figure 2 shows a linear dependence of the chemiluminescence on the M_2 density. Furthermore, it is evident that it is $O(^3P)$ which takes part in the light producing process, since $O(^3P)$ is the only species which both oxygen sources described above produce in common. (Weak chemiluminescence was also observed when the alkali beams were crossed with O_2. It was strongest with Cs. In general, the chemiluminescence was weaker than in the case of the reactions with O by a factor of 10^2 to 10^3. The luminescence mainly consisted of alkali resonance lines.) Figures 2 and 3 show that the reaction is of first order with respect to M_2 and $O(^3P)$.

To determine the order of magnitude of the cross sections for the reactions investigated, we compared them to those of the reactions

$$M_2 + Cl_2 \rightarrow MCl + Cl + M^* . \qquad (6)$$

For this purpose, the O beam was substituted by a Cl_2 beam and the chemiluminescence from Reaction (6) was measured. Results for the ratios of the cross sections of Reactions (5) and (6) derived from these measurements are given in Table I. Struve *et al.* report a cross section between 0.3 and 3 Å² for Reaction (6)[4] in the case M = K. By comparison, we infer a cross section between 0.66 and 6.6 Å² for Reaction (5) (M = K) studied here.

The spectrum of the chemiluminescence of Reaction (5) was investigated. The detection system allows measurements in the range from 2500 to 9000 Å. With Na_2,

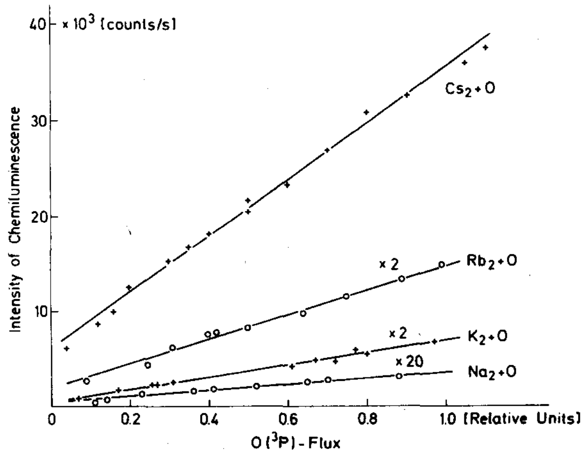

FIG. 3. Chemiluminescence intensity versus the $O(^3P)$ flux. The $O(^3P)$ atoms were generated by the rapid reaction NO+N $\rightarrow N_2 + O(^3P)$. Their flux was indirectly determined by measuring the NO flux with a flowmeter.

TABLE I. Experimental cross sections for the chemiluminescent reaction $M_2 + O \rightarrow MO + M^*$ in comparison to those of $M_2 + Cl_2 \rightarrow MCl + Cl + M^*$. (In the case M = Na, the reaction $M_2 + Cl_2 \rightarrow MCl + Cl + M^*$ is endothermic. At present, we do not know what process is responsible for the observed luminescence.) In this study, the chemiluminescence was not spectrally resolved.

M_2	$\sigma(M_2+O)/\sigma(M_2+Cl_2)$
Na_2	2.5
K_2	2.2
Rb_2	4.5
Cs_2	3.8

K_2, and Rb_2 as reactants, the spectra contained only the fundamental resonance lines (Fig. 4). These are the transitions which may be observed due to exoergicity. In the case of the reaction with Cs_2, the spectrum of the chemiluminescence again mainly consisted of the fundamental resonance lines. In addition, the luminescence also contained the transitions from the 7p doublet to the ground state and the 6d $^2D_{3/2}$–6p $^2P_{1/2}$ transition. The latter lines were about 10^{-3} times weaker than the fundamental resonance lines. The finding that the 6d $^2D_{3/2}$ level is also populated by the reaction suggests the possibility that also thermal energy of the reactants is converted into electronic energy of the products, since this level lies much higher than the exoergicity boundary. No molecular lines were observed. If the product alkali monoxide MO is excited, the chemiluminescence is in the infrared.[8] This, however, cannot be observed by our detection system.

Efforts to enhance the production rates for levels near the exoergicity boundary by exciting the reactants $M_2(M_2 = K_2, Rb_2)$ electronically and also vibrationally via Franck–Condon pumping by krypton and dye lasers have shown no success so far. This may simply be due to the fact that only a very small fraction of the reacting M_2 could be excited.

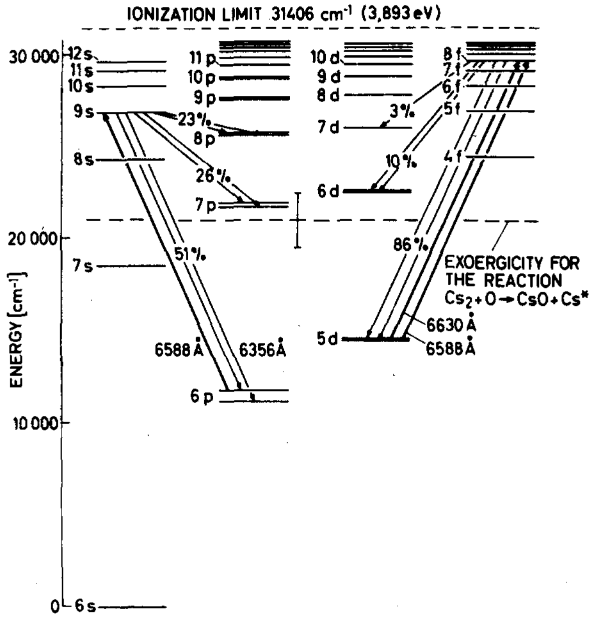

FIG. 5. Laser induced transitions (thick arrows) and fluorescence channels (thin arrows) used for the determination of the detailed rate constants of the 5d levels of the product Cs atoms. Transitions from and to the 6p level were used for calibration.

For a more detailed study of the reaction mechanism (5), we have to determine the detailed rate constants for the production of the states below the exoergicity limit of the product atom.

In the case of Cs, the detailed rate constants for the production of the states 6p $^2P_{1/2,3/2}$, 7p $^2P_{1/2,3/2}$, and 6d $^2D_{3/2}$ can be deduced from the chemiluminescence intensity. Radiation from 5d $^2D_{3/2,5/2}$ and 7s $^2S_{1/2}$ lies in the infrared and cannot be measured by our detection system. Therefore, we had to apply the method of laser

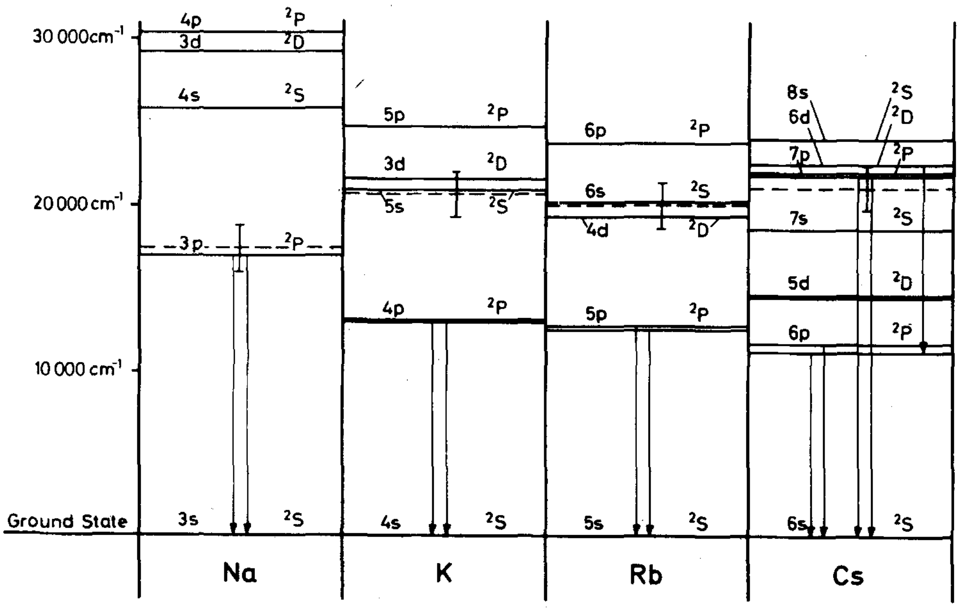

FIG. 4. Low lying levels of the product alkali atoms M^* of the reactions $M_2 + O \rightarrow MO + M^*$. The dashed lines indicate the exoergicities of the reactions, i.e., the differences of the bonding energies of MO and M_2[8,11] neglecting thermal energy. The arrows indicate the transitions observed in chemiluminescence.

induced fluorescence (LIF) to investigate the population of those states. To measure the density of product atoms in the state $5d\,^2D_{3/2}$, a transition was induced to the $8f\,^2F_{5/2}$ state using a single mode laser working with the dye Rhodamine 101 as lasing medium (Fig. 5). The resonance fluorescence from $8f\,^2F_{5/2} \rightarrow 5d\,^2D_{3/2}$ was measured using an interference filter to suppress the background radiation from the chemiluminescence. Since the transition probabilities involved are known,[10] the density of the $5d\,^2D_{3/2}$ level can be calculated from the intensity of the fluorescence. In a similar way, the $5d\,^2D_{5/2}$ level was investigated as shown in Fig. 5.

Since we had to compare the LIF results to the chemiluminescence measurements, for calibration a LIF experiment on the $6p\,^2P_{3/2}$ state was performed. For this purpose, the transition from the $6p\,^2P_{3/2}$ to the $9s\,^2S_{1/2}$ state was induced (Fig. 5).

The population densities determined in this way are converted into detailed rate constants using the lifetime of the states. The results of the LIF measurements are compiled in Table II. The transition probabilities needed for the evaluation of the LIF data were taken from Agnew.[10] Optical pumping during the LIF measurements may falsify slightly the results. The effect was at most a few percent on the reaction rates since the laser beam intensity was kept as low as 0.5 mW/cm².

Though the detailed rate constant for the upper $5d\,^2D_{5/2}$ state is smaller than that of the lower lying $6p\,^2P_{3/2}$ state (Table II), the density of product atoms in the upper state is larger than in the lower one by a factor of 1.8. This is mainly due to the long lifetime of 1.1 μs of the $5d$ levels compared to 33 ns of the $6p$ levels. The ratio of 1.8 means a population inversion of the two levels.

An attempt was made to measure the rate for the production of ground state Cs atoms by Reaction (5). A LIF experiment was performed using a Stilbene 3 dye laser to probe the transition $6s\,^2S_{1/2} \rightarrow 7p\,^2P_{1/2}$. The discharge producing the O beam was modulated and, with the phase sensitive detector, it was searched for a modulation in the laser induced fluorescence. It was not possible to discriminate between the ground state atoms from the reaction and those from the reactant alkali beam.

In Fig. 6, the detailed rate constants of all the states investigated in this work are plotted versus the excitation energy of the states.

TABLE II. Results of the LIF measurements on the $5d$ doublet. N are the densities and P the detailed rate constants.

$\frac{N(5d\,^2D_{3/2})}{N(6p\,^2P_{3/2})} = 0.8\ (3)$	$\frac{P(5d\,^2D_{3/2})}{P(6p\,^2P_{3/2})} = 0.022\ (8)$
$\frac{N(5d\,^2D_{5/2})}{N(6p\,^2P_{3/2})} = 1.8\ (5)$	$\frac{P(5d\,^2D_{5/2})}{P(6p\,^2P_{3/2})} = 0.040\ (16)$

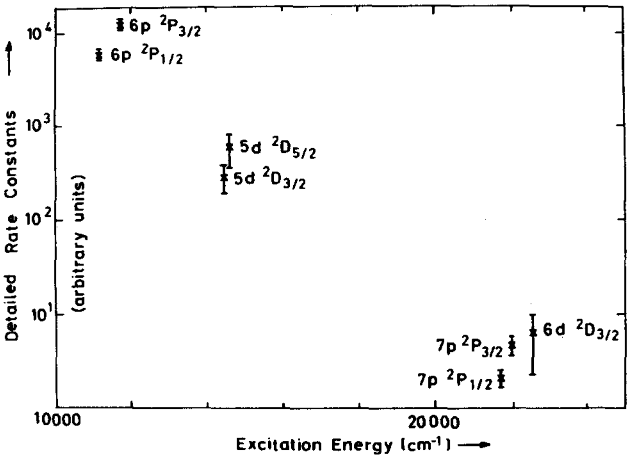

FIG. 6. Logarithm of the detailed rate constants for the Cs product atomic states as a function of the excitation energy. In the case of the $6p$, $7p$, and $6d$ states, the error bars mainly represent the uncertainties resulting from photon counting statistics. The error bars given for the detailed rate constants of the $5d$ states additionally include uncertainties due to signal fluctuations by laser intensity fluctuations. Furthermore, the uncertainties of the transition probabilities used in the evaluation[10] were added.

DISCUSSION

It is interesting to compare the results for the dimer-oxygen reactions investigated in this paper to the dimer-hydrogen and dimer-halogen reactions, which are formally similar:

$$M_2 + H \rightarrow MH + M\ , \tag{7}$$

$$M_2 + X \rightarrow MX^* + M^*\ , \tag{8}$$

where H = hydrogen atom, X = halogen atom, and the asterisks in Reaction (8) refer to an electronic excitation. Reactions (7) and (8) have also been investigated in crossed beam experiments. Reaction (7) was studied by Lee *et al.*[11] In this case no visible luminescence has been observed. However, for Reaction (8), the products MX and M showed chemiluminescence as was found by Struve *et al.*[4]

The reaction paths of Reactions (7) and (8) are in good agreement with the expectation according to schematic adiabatic state correlation diagrams. In the diagrams shown in Figs. 7(a) and 7(b), it is assumed that a bent reaction complex M_2H and M_2X, respectively, of the symmetry group C_s is formed. According to Fig. 7(a), only one reaction path starts from the reactants' ground state $M_2(^1\Sigma_g) + H(^2S_g)$ to the complex M_2H and it yields the products MH + H in their ground states, in agreement with the experiment of Lee *et al.*

In the case of the reaction $M_2 + X$, three potential surfaces belong to the reactants in the ground state $M_2(^1\Sigma_g)$ and $X(^2P_u)$ as shown in Fig. 7(b). One of them ($^2A'$) leads to the products in their ground state $MX(^1\Sigma^+) + M(^2S_g)$. However, the other two ($^2A'$ and $^2A''$) lead to an excited state $MX(^1\Sigma^+) + M^*(^2P_u)$. This is in accordance with the experiment of Struve *et al.*, where the

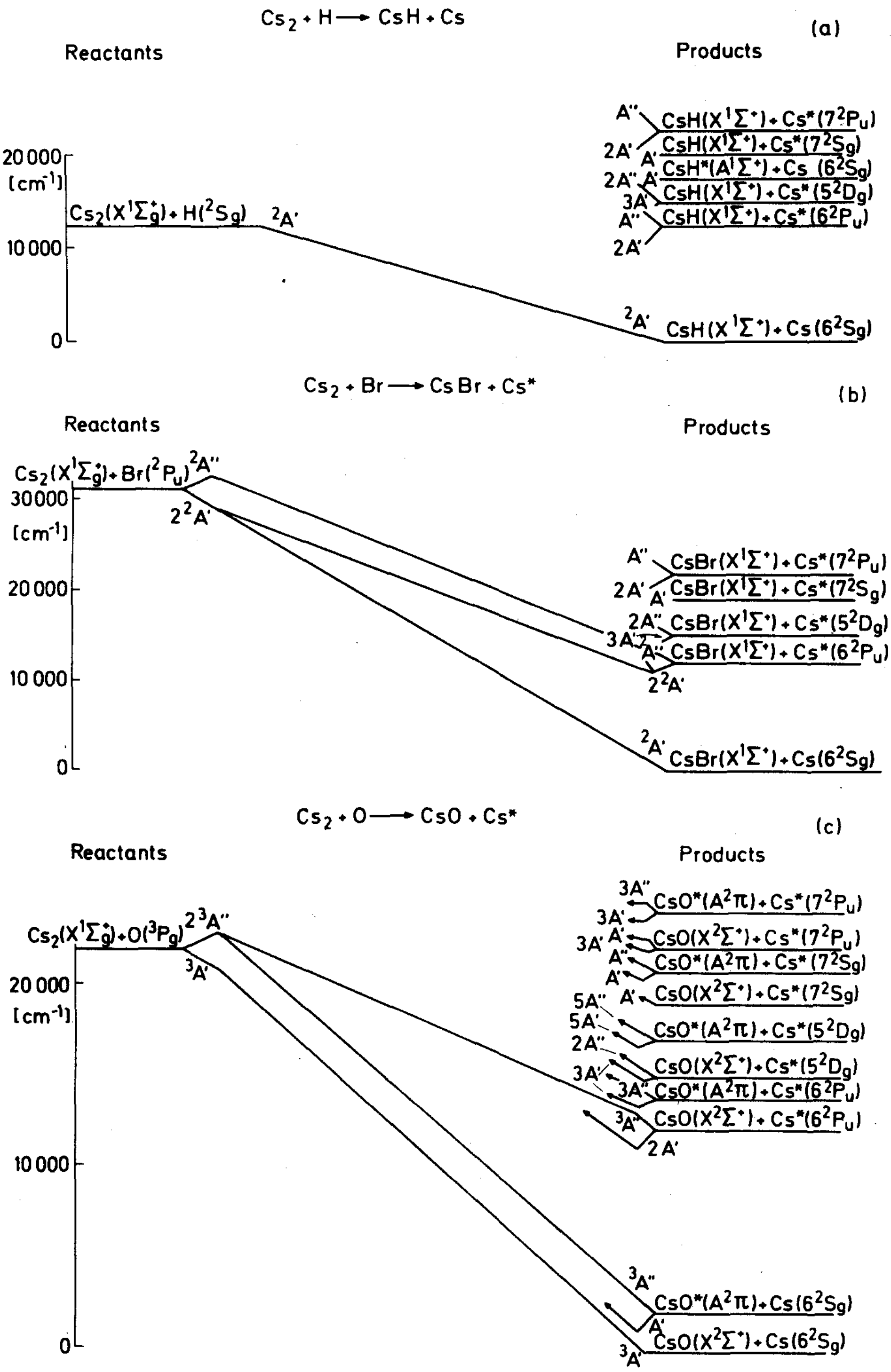

FIG. 7. Adiabatic state correlation diagrams of the reactions between Cs dimers and H, Br, and O. The states of the intermediate complexes are not known. Therefore, they are omitted in the diagrams.

alkali *D* lines were found to give the main contribution to the luminescence observed.

The correlation diagram of the reaction $M_2 + O$ studied in this paper as shown in Fig. 7(c) has to be compared to the $M_2 + H$ and $M_2 + X$ diagrams just discussed. As in the $M_2 + X$ case, three surfaces start from $M_2(^1\Sigma_g) + O(^3P_g)$. One of them (of the species $^3A'$) leads to the products ground state $MO(^2\Sigma^+) + M(^2S_g)$, similar to the diagram of the reaction $M_2 + X$. However, only one potential surface leads to the excited product state $MO(^2\Sigma^+) + M^*(^2P_u)$. In accordance with this, our experiments showed a weaker *D*-line emission in the reaction $M_2 + O$ than in the $M_2 + X$ case.

The third surface of the species $^3A''$ leads to $MO^*(^2\Pi) + M(^2S_g)$, i.e., to an excited molecule; however, radiation from this state cannot be observed in our experiment as mentioned before.

More insight into the details of the reaction studied here is obtained by considering the detailed cross sections for the production of the different electronic states of Cs. In Fig. 8, the logarithm of the detailed cross

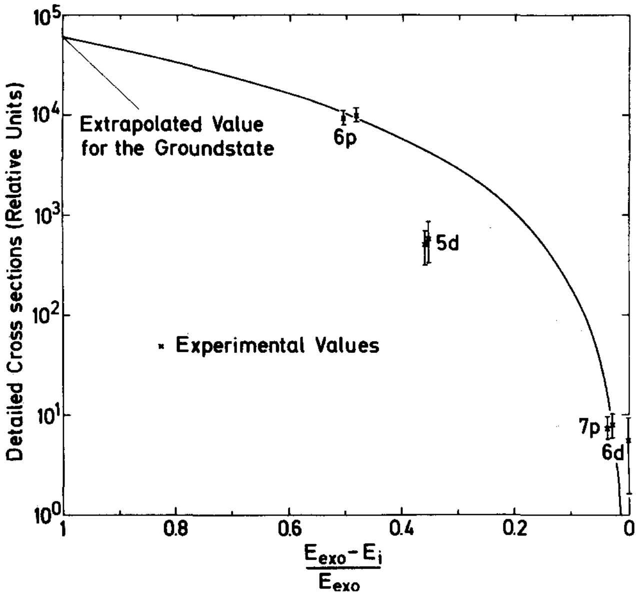

FIG. 8. Experimental detailed cross sections for the product atomic states in comparison with the microcanonical distribution (continuous curve). The experimental cross sections in this figure were taken to be proportional to the rate constants of Fig. 6.

sections for the states investigated, divided by the statistical weights $g=2J+1$ of these states, is plotted versus E_i-E_{exo}, where E_i is the excitation energy of the state i and E_{exo} the overall exoergicity. The values for all the doublets nearly coincide in this plot. This means that the detailed cross sections of electronic states belonging to the same multiplet are roughly proportional to the statistical weights.

In this aspect, the reaction investigated resembles closely the alkali dimer–halogen atom reaction (8). For this case, Struve *et al.*[4] found a nearly statistical distribution of the product alkali atoms over the energetically accessible excited states. They explained this result by the multitude of avoided crossings between ionic and covalent potential energy surfaces in this system. As a consequence, the flow of the energy should be essentially unrestricted.

Krenos and Tully[12] found that the distribution of the M* from Reaction (8) over the energetically accessible electronic states could be described even better by statistical phase space theory of Pechukas *et al.*[13] Here the relative cross sections $\sigma(E_i)$ for the states i with excitation energy E_i are described by

$$\sigma(E_i)=\alpha g_i(E_{exo}-E_i)^{\beta} , \qquad (9)$$

where g_i is the statistical weight of state i, E_{exo} is the overall exoergicity, and α and β are constants. The result of the least squares fit to the experimental data is that β equals about 2, in accordance with phase space theory.[12]

An equation of exactly the same form as Eq. (9), but with

$$\beta=(t+r)/2+v-1 , \qquad (10)$$

describes a microcanonical product state distribution.[14] Here, t, r, and v denote, respectively, the number of translational, rotational, and vibrational degrees of freedom of the products. In our case (atom–diatom), $t=3$, $r=2$, and $v=1$; hence, $\beta=5/2$. The curve in Fig. 8 displays the microcanonical distribution as calculated by Eqs. (9) and (10) together with our experimental points. The constant α in Eq. (9) was adjusted so that the experimental value for $\sigma(6p\,^2P_{1/2})$ lies on the curve. For E_{exo}, we took the excitation energy of the state $6d\,^2D_{3/2}$. This was the highest excited product state in Reaction (5). The $J=5/2$ state of the same doublet, which lies only 42 cm^{-1} higher, was not excited.

As we see from Fig. 8, the experimental values for $\sigma(7p\,^2P_{1/2})$ and $\sigma(7p\,^2P_{3/2})$ nearly coincide with the theoretical curve. This means that the population ratio of the $6p$ and $7p$ doublets occurs statistically by the reaction. However, for the $5d$ doublet we find a population lower by an order of magnitude compared to the statistical distribution as given by the curve in Fig. 8. This indicates that there are also dynamical constraints in the system which impede a free flow of the energy between the electronic and possibly other degrees of freedom. The schematic correlation diagram gives us no indication why the $5d$ doublet is anomalous.

The consequences of this partly unstatistical distribution are that more than 95% of the excitation is channeled into the $6p$ doublet states. This suggests using this system to pump an alkali dimer laser. It is well known that the cross sections for energy transfer from

TABLE III. Summary of reaction cross sections for M_2+O.

Reactants	E_{exo} (kcal/mol)[a]	$E(^2P_{1/2})$ (kcal/mol)	$\sigma(\text{gr})/\sigma(^2P_{1/2})$	σ_{tot}^{exp} (Å^2)	I. P. – E. A. (eV)	R_x (Å)	σ_{tot}^{harp} (Å^2)
Na_2+O	54.5	48.5	83	2.1⋯21	3.4	4.2	55
K_2+O	62.2	37.3	3.3	4.0⋯40	2.5	5.7	103
Rb_2+O	60.9	36.6	3.3	9.9⋯99	2.4	6.0	111
Cs_2+O	64.6	33.1	2.0	13.5⋯135	2.3	6.2	120

[a] The exoergicity E_{exo} is calculated as the difference between bonding energies of the product molecule MO (Ref. 8) and the reagent molecule M_2 (Ref. 11) plus the kinetic energy of the reactants in the c.m. system. This grows from 0.6 to 1.6 kcal/mol in the row from Cs_2 to Na_2. The ionization potentials (I.P.) are taken from the tables of Huber and Herzberg.[18] For the electron affinity (E.A.) of the oxygen atom, the value 1.47 eV measured by photon detachment[19] was taken. R_x is the distance at which the electron jump from the alkali dimer to the oxygen atoms occurs. σ_{tot}^{exp} is the experimental cross section which is to be compared to σ_{tot}^{harp}, the cross section predicted by the harpoon model.

alkali atoms excited to the lowest ^2P states to the alkali dimers are large. In particular, Ham and Heavens[15] showed in a heat pipe experiment with sodium that only a few rovibronic levels of the $A\,^1\Sigma_u$ state of Na_2 were excited by trapping the photons radiated by $Na(3p\,^2P)$. The $Na(3p\,^2P)$ atoms were created by Reaction (8). The inversion in this system was between the populated states of the $A\,^1\Sigma_u$ of Na_2 and higher lying rovibronic levels of the ground state.

Since the experimental values for the detailed cross sections show at least partial agreement with those calculated from statistical theory, as shown in Fig. 8, it looks promising to extrapolate the curve to $E_i = 0$ to get a detailed cross section $\sigma(\mathrm{gr})$ for the ground state. In this manner, for all the $M_2 + O$ reactions investigated in this paper, $\sigma(\mathrm{gr})$ was obtained by the formula

$$\frac{\sigma(\mathrm{gr})}{\sigma(^2P_{1/2})} = \frac{g(\mathrm{gr})}{g(^2P_{1/2})}\left[\frac{E_{exo}}{E_{exo} - E(^2P_{1/2})}\right]^{5/2} . \qquad (11)$$

Here, $^2P_{1/2}$ always designates the lowest lying $^2P_{1/2}$ state. Values used for E_{exo} and $E(^2P_{1/2})$ as well as for $\sigma(\mathrm{gr})$ are displayed in Table III. In order to obtain $\sigma(\mathrm{gr})$, $\sigma(^2P_{1/2})$ was derived from the cross section ratios in Table I and the absolute value for the cross section of the $K_2 + Cl_2$ reaction given by Struve *et al.*[4]

Total absolute cross sections are obtained by summing the detailed cross sections values [as shown above, only the contributions of $\sigma(\mathrm{gr})$ and $\sigma(^2P_{1/2})$ have to be considered]

$$\sigma_{\mathrm{tot}}^{\mathrm{exp}} \approx \left[\frac{\sigma(\mathrm{gr})}{\sigma(^2P_{1/2})} + 1\right]\sigma(^2P_{1/2}) . \qquad (12)$$

Results are listed in Table III.

Total cross sections measured for the alkali–halogen reactions could be interpreted successfully by the harpoon model of Polanyi[16] and Magee.[17] Since Lindsay *et al.*[9] found that the bonding in MO is predominantly ionic like in MX and MH, the experimental results of this paper can also be compared to the harpoon model. Absolute cross sections are given herein by

$$\sigma_{\mathrm{tot}}^{\mathrm{harp}} = \Pi R_x^2 , \qquad (13)$$

where R_x is the distance at which the electron jump from the alkali dimer to the oxygen atom occurs. Therefore, R_x is determined by

$$R_x = \frac{e^2}{\mathrm{I.P.} - \mathrm{E.A.}} = \frac{14.4\ \text{Å eV}}{\mathrm{I.P.} - \mathrm{E.A.}} , \qquad (14)$$

where I.P. is the ionization potential of the alkali dimer and E.A. the electron affinity of the oxygen atom.

From Table III we see that the cross sections derived from the harpoon model using Eq. (13), i.e., $\sigma_{\mathrm{tot}}^{\mathrm{harp}}$, agree very well with the upper limits of $\sigma_{\mathrm{tot}}^{\mathrm{exp}}$ (for Rb_2 and Cs_2). In the cases of Na_2 and K_2, $\sigma_{\mathrm{tot}}^{\mathrm{harp}}$ is found to be too large by a factor of 2.5 compared to $\sigma_{\mathrm{tot}}^{\mathrm{exp}}$. The trend of $\sigma_{\mathrm{tot}}^{\mathrm{exp}}$ increasing in the series from Na_2 to Cs_2 is displayed correctly. Furthermore, it is noticeable that the ratio of the experimental cross sections of the $M_2 + O$— and the $M_2 + X$—reactions is described by the harpoon model fairly well.

ACKNOWLEDGMENTS

We are indebted to H. Shugart and F. Franz for their help in the LIF measurements and to A. Ben Shaul for discussions in statistical theory. We are grateful to H. Käsbauer and K. Stockinger for their technical assistance.

[1] See, for example, S. Chapman, Astrophys. J. 90, 309 (1939).
[2] M. Ogawa, Sci. Light 3, 47 (1954).
[3] D. Golomb, H. S. Hoffman, and G. T. Best, J. Geophys. Res. 80, 1363 (1975).
[4] W. S. Struve, J. R. Krenos, D. L. McFadden, and D. R. Herschbach, J. Chem. Phys. 62, 404 (1975).
[5] W. S. Struve, Mol. Phys. 25, 777 (1973).
[6] See, for example, J. Wolfrum, "Atom Reactions," in *Physical Chemistry* (Academic, New York, 1975), Vol. VIB.
[7] R. J. Gordon, Y. T. Lee, and D. R. Herschbach, J. Chem. Phys. 54, 2392 (1971).
[8] R. R. Herm and D. R. Herschbach, J. Chem. Phys. 52, 5783 (1970).
[9] D. M. Lindsay, D. R. Herschbach, and A. L. Kwiram, J. Chem. Phys. 60, 315 (1974).
[10] L. Agnew and C. Summers, Proceedings of the 7th International Conference on Phenomena in Ionized Gases, Belgrade (1965), Vol. II, p. 574; see also M. Fabry, J. Quant. Spectrosc. Radiat. Transfer 16, 127 (1976).
[11] Y. T. Lee, R. J. Gordon, and D. R. Herschbach, J. Chem. Phys. 54, 2410 (1971).
[12] J. R. Krenos and J. C. Tully, J. Chem. Phys. 62, 420 (1975).
[13] P. Pechukas, J. C. Light, and Ch. Rankin, J. Chem. Phys. 44, 794 (1966).
[14] W. Forst, *Theory of Unimolecular Reactions* (Academic, New York, 1973).
[15] D. O. Ham and C. T. Havens, in *Electronic Transition Lasers*, edited by Steinfeld (MIT, Cambridge, Mass., 1976).
[16] M. Polanyi, *Atomic Reactions* (Williams and Norgate, London, 1932).
[17] J. L. Magee, J. Chem. Phys. 8, 687 (1940).
[18] K. P. Huber and G. Herzberg, *Molecular Spectra and Molecular Structure* (Van Nostrand Reinhold, New York, 1978), Vol. IV.
[19] M. Karplus and R. N. Porter, *Atoms and Molecules* (Benjamin, New York, 1970).